Continuous 16.4-THz Bandwidth Coherent DWDM Transmission in O-band using a Single Fibre Amplifier System

Daniel J. Elson, Mindaugas Jarmolovičius, Vitaly Mikhailov, *Member, IEEE*, Jiawei Luo, Daryl Inniss,
Shohei Beppu, Glenn Baxter, Ralf Stolte, Luke Stewart, Shigehiro Takasaka, Eric Sillekens, Robert I. Killey,
Polina Bayvel, *Fellow, IEEE*, Noboru Yoshikane, Takehiro Tsuritani, *Senior Member, IEEE*,
Yuta Wakayama, *Member, IEEE*

(Invited Paper)

Abstract—A record continuous transmission bandwidth of 16.4 THz is demonstrated in O-band fibre transmission over an 80-km single-mode ultra low-loss fibre span. Bismuth-doped fibre amplifiers with an output power of 25 dBm and a low noise figure of 3.6 dB compensate a loss of 80-km fibre span. An O-band wavelength selective switch with a 16.4 THz bandwidth maximises the transmission capability and enabled optimisation of the input spectrum shape to reduce nonlinear interference near zero dispersion, resulting in a potential achievable information rate of over 100 Tb/s to be reached.

Index Terms—Optical fibre communication, coherent dense wavelength division multiplexing, O-band, bismuth doped fibre amplifier (BDFA).

I. INTRODUCTION

CONSIDERING the continuous surge in data traffic for artificial intelligence services, bandwidth requirements especially for data centre interconnects (DCIs) have been rapidly increasing [1]–[3]. To address these demands, ultra-wideband transmission experiments have been reported that utilise multiple bands [4]–[7]. The largest transmission bandwidth, 37 THz, was demonstrated in the O+E+S+C+L+U-band over 50 km, using five different types of fibre amplifiers, incorporating a distributed Raman pumping scheme, along with bismuth-, thulium-, and erbium-doped fibre amplifiers (O-band BDFAs, E-band BDFAs, S-band TDFAs, C-band EDFAs, L-band EDFAs and discrete U-band lumped Raman amplifiers). A greater distance of 100 km was also achieved [8] but required the total transmission band to be reduced below 36 THz due to a combination of amplifier gain, fibre loss and inter-channel stimulated Raman scattering (ISRS). The throughput was potentially limited by the use of band (de)multiplexers and ISRS, especially at shorter wavelengths. By way of a possible simplification to the transmission system, ultrawideband configurations using only a single type of amplifier without band (de)multiplexers have been proposed [9], and a transmission bandwidth of 12.5 THz across the S+C+L-band demonstrated using an ultrawideband semiconductor optical amplifier. This required the use of free space optics to support polarisation multiplexed signals and had an average noise figure above 6 dB. A more attractive lower noise amplifier solution is O-band BDFAs which have been shown to have gain bandwidths in excess of 10 THz [10], [11]. Nevertheless, high capacity transmission in the O-band was not considered as feasible due to higher nonlinear interference noise (NLIN) around the zero dispersion wavelength [12], [13]. A transmission bandwidth of 9.6 THz in the O-band using a simple O-band BDFA was experimentally investigated [14]. Although the bandwidth was equivalent to that of the C+L-band, the O-band has even greater potential with a bandwidth of beyond 17 THz [15]. This band is defined from the start of single mode operation of single mode fibre (the cut off wavelength 1260 nm) to the increase in loss due to water peak in conventional G.652.A fibres (from 1360 nm), as seen in Table I which in terms of wavelength is only 100 nm in bandwidth but in terms of frequency is 17.5 THz. Prior work has not fully utilised this single band, and in this work, we demonstrate a record transmission bandwidth of 16.4 THz, approaching the maximum possible, using a single optical amplifier system. This was enabled by three key technologies. Firstly, ultrawideband high-power BDFA, secondly, a WSS, and thirdly, spectrally-shaped power optimisation, which simultaneously mitigated

D. J. Elson, S. Beppu, Y. Wakayama, N. Yoshikane, and T. Tsuritani are with KDDI Research, 2-1-15 Ohara, Fujimino, Saitama, 356-8502, Japan (e-mail: xda-elson@kddi.com; sh-beppu@kddi.com; da-souma@kddi.com; yu-wakayama@kddi.com; no-yoshikane@kddi.com; ta-tsuritani@kddi.com).

V. Mikhailov and J. Luo are with OFS Laboratories, 19 Schoolhouse Rd., Somerset, New Jersey 08873, USA (e-mail: vmikhailov@ofsoptics.com; jluo@ofsoptics.com).

G. Baxter, R. Stolte and Luke Stewart are with Finisar Australia, 21 Rosebery Ave, Rosebery, NSW 2018, Australia (email: glenn.baxter@finisar.com; ralf.stolte@finisar.com; luke.stewart@finisar.com)

S. Takasaka is with Furukawa Electric Co., Ltd., 6 Yawata-kaigandori, Ichihara 290-8555, Japan (email: shigehiro.takasaka@furukawaelectric.com)

D. Inniss, formerly OFS Laboratories, is now with InnissCom, Colorado 80027, USA (e-mail: drinniss@gmail.com)

M. Jarmolovičius, E. Sillekens, R. I. Killey and P. Bayvel are with Optical Networks Group, UCL (University College London), London (email: zceemja@ucl.ac.uk; e.sillekens@ucl.ac.uk; r.killey@ucl.ac.uk; p.bayvel@ucl.ac.uk)

Band	Wavelength (nm)	Bandwidth (THz)
O	1260–1360	17.5
E	1360–1460	15.1
S	1460–1530	9.4
C	1530–1565	4.4
L	1565–1625	7.1
U	1625–1675	5.5

TABLE I: The standard operating bands with wavelength ranges and corresponding bandwidths

both nonlinear interference noise (NLIN) and ISRS over the O-band. The high-power BDFA exhibits more than 6-dB gain bandwidth of over 17 THz and was used to increase the signal power in transmission over an 80.4-km unrepeated link. The ultrawideband wavelength selective switch (WSS) enabled us to shape the spectrum to mitigate both the ISRS power transfer and reduce the NLIN penalty near the zero dispersion frequency (ZDF). The power profile was optimised using the Gaussian noise (GN) model [16]. To our knowledge, this is the first investigation of the wideband transmission performance and degradation due to the ISRS and NLIN around the ZDF.

II. TRANSMISSION EXPERIMENT CHARACTERISATION

In order to generate signal loading across the whole the O-band, a programmable filter was used to generate spectrally shaped ASE. Here, a wavelength selective switch (WSS) used in this experiment has an operating frequency range from 220.76 THz to 237.20 THz and a minimum filter bandwidth of 30 GHz, maximum attenuation of 40 dB, with a nominal loss of 8 dB. This was used to flatten the gain spectrum, correcting for ISRS and to carve a notch for the channels under test.

Amplification was provided by BDFAs in two configurations, co- and counter-pumped. The BDFAs were characterised using an ASE comb carved from an ASE source. A superluminescent diode (SLED) was used as an ASE seed source, and amplified by a BDFA. Using the WSS, the spectrum was flattened and carved into 50 GHz channels on a 150 GHz grid, to achieve a minimum OSNR of 26.1 dB. This enabled a 53-point WDM characterisation of the BDFA. The total power input to the BDFA under test was set to -1 dBm with variable optical attenuators, resulting in an input power of -18 dBm per channel. This total input power is the expected input power after fibre transmission but not including the expected loss profile. The input and output spectra of the BDFA were measured using an OSA set to a resolution of 0.1 nm and compared to calculate the gain and noise figure. Two BDFA configurations were tested, co- and counter- pumped and the results can be seen in Fig. 1(a) and (b), respectively. The pump wavelength into 250 m of BDF was 1150 nm. This came from a YDF conversion stage converting from a 915 nm multi mode laser diode [10]. The co-pumped BDFA used a laser pump current of 4.5 A and the counter-pumped a current of 4.0 A. The average and peak gain values were 21.2, 22.9 dB and 21.0, 23.0 dB with average noise figures of 3.6 and 4.8 dB, for the co- and counter pumped configurations, respectively. Only one amplifier was in the co-pumped configuration and
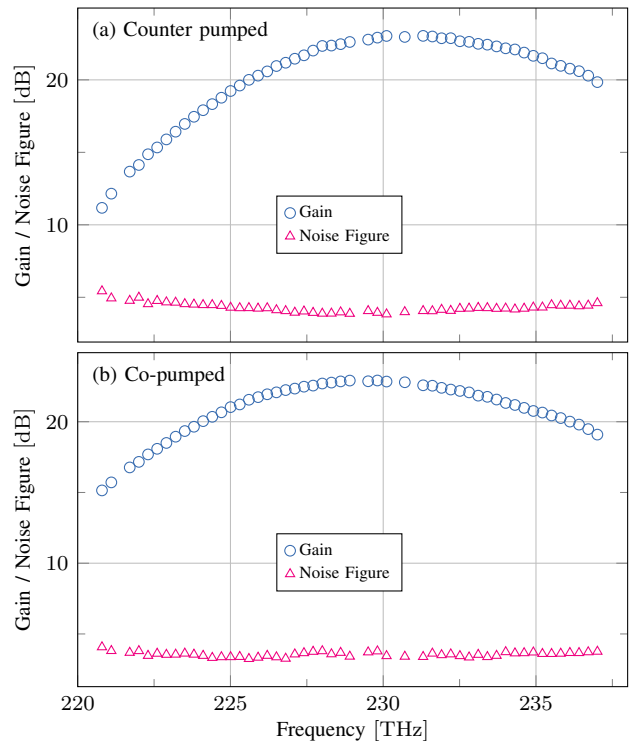

Fig. 1: The gain and noise figure measured as a function of frequency for both (a) counter and (b) co-pumped configurations. WDM measurements were performed on an ASE comb with fixed total input power of -1 dBm

from here on this is referred to as a pre-amplifier due to its lower noise characteristics.

III. ISRS CHARACTERISATION

The combination of high input powers and increasing transmission bandwidths can lead to significant amounts of ISRS that can impact transmission throughput [17]. This phenomenon shifts power from higher to lower frequencies (shorter to longer wavelengths) and can be seen effectively as an increase and reduction in apparent fibre loss for higher frequencies and lower frequencies, respectively. We next experimentally verified the model used in [18] in the O-band over 17.4 THz.

The transmission link was 80.4 km long and consisted of five reels of AllWave® ULL single-mode optical fibre, compliant with ITU-T G.652.B. The measured total loss and dispersion profile is shown in Fig. 2, where the ZDF was measured to be 228.90 THz (1309.71 nm). The low loss characteristics mean that the average loss for the span across all transmission wavelengths was 0.32 dB/km with a total loss of 24 and 30 dB at 220 and 238 THz, respectively. In Table II, the zero dispersion values for each reel are listed as well as the combined value, which was measured after splicing all the reels together.

The input and output spectra were measured for various launch powers and the difference was taken to calculate the apparent loss of the fibre and this is shown in Fig. 3(a). Dashed lines show the expected spectrum after solving the differential equations. When the total input power was within the range of
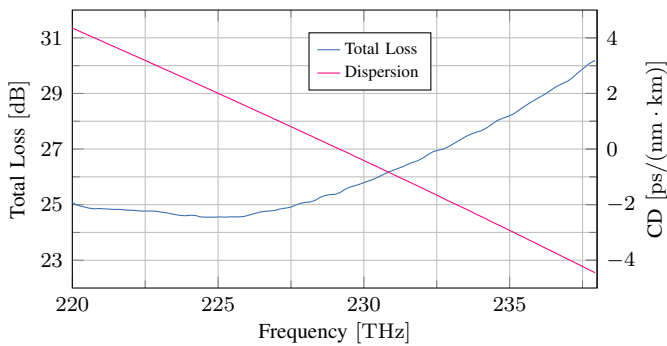
Fig. 2: Fibre characteristics: dispersion and loss profiles as a function of frequency for a single 80.4 km span of ultra-low loss fibre.

10-16 dBm (-15 to -9 dBm/channel), the apparent fibre loss changed by less than 1 dB, but after increasing the launch power beyond 16 dBm, significant power transfer from high to low frequencies started to occur. For an input power of 22 dBm, the apparent fibre loss at the higher frequency of 238 THz increased by 2.6 dB and the apparent fibre loss at the lower frequency 220 THz was reduced by 2.7 dB, leading to a power transfer of 5.4 dB. This behaviour continued, as the launch power was increased; even greater variations in apparent loss occurred. By subtracting the loss of the fibre at the lowest input power where no ISRS is observed, the ISRS can be quantified, as shown in Fig. 3(b). For launch powers lower than 14 dBm, the total tilt across the whole transmission bandwidth is less than 1 dB. However, at launch powers greater than 22 dBm, there is more than 5 dB of power transferred from the higher frequencies to the lower frequencies.

The maximum power transfer from ISRS can be approximated using a triangular gain profile up to 15 THz as [18],

$$\Delta P = 4.3 \cdot P_{\text{tot}} C_r L_{\text{eff}} B, \tag{1}$$

where the attenuation was $\alpha = 0.32$ dB/km, assumed Raman gain coefficient $C_r = 0.033$ 1/W $\cdot$ THz $\cdot$ km, $L = 80.4$ km, nonlinear effective length: $L_{\text{eff}} = (1 - \exp(-\alpha L))/\alpha = 14.4$ km, total launch power $P_{\text{tot}} = 26$ dBm and bandwidth $B = 16.4$ THz. The expected ISRS power transfer reaches 13.5 dB. This equation was previously shown to be valid for bandwidths up to 10 THz [17]. Subtracting the minimum and maximum values on of each measurement in Fig. 3(b), the maximum ISRS power transfer can be measured as a function of input power. This is shown in Fig. 4. The measured power tilt for the maximum input power of 26 dBm was

Subspan	Zero Dispersion Wavelength (nm)	Zero Dispersion Frequency (THz)
1	1309.2	228.99
2	1310.0	228.84
3	1308.8	229.06
4	1311.1	228.66
5	1305.8	229.58
Combined	1309.7	228.94

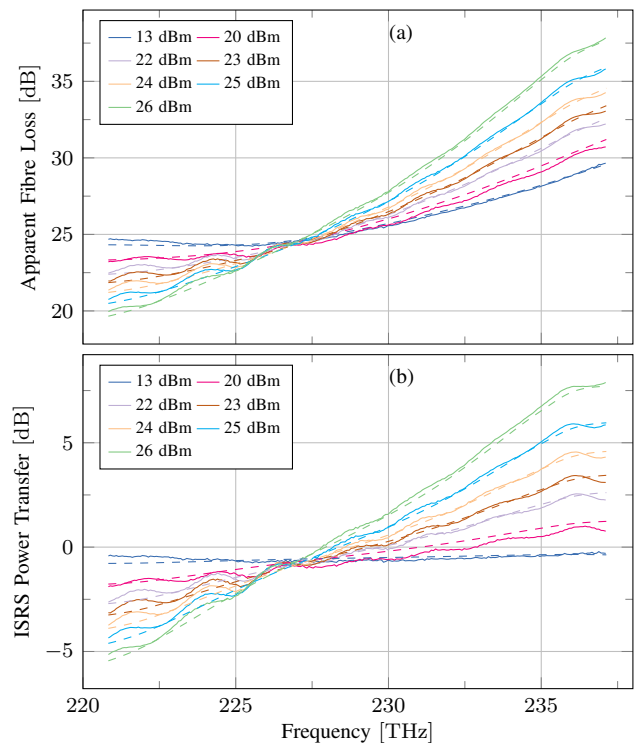TABLE II: The zero dispersion wavelength and frequencies for each subspan of the 80.4 km link

Fig. 3: (a) Apparent fibre loss and (b) measured ISRS power transfer as a function of frequency for considered launch powers equivalent to -12 - $+1$ dBm/channel. Dashed lines are model estimation obtained by solving Raman ODEs.

13.1 dB (-0.1 dBm/chan), whereas it was only 5.4 dB for an input power of 22 dBm (-3.1 dBm/chan). The experimental and analytical values differ by only 0.4 dB demonstrating the validity of Eqn. 1 beyond 15 THz. Initially a simple compensation of the ISRS is attempted. An expected tilt of 5.4 dB was calculated. This tilt was inverted and applied to the WSS in addition prior BDFA flattening shape. This launch power compensation is seen in Fig. 6 labelled as ISRS compensation. The gain of the subsequent BDFA was nonlinear and this meant that a simple 5.4 dB slope was not observed. The ISRS power transfer was also modelled by solving Raman ordinary differential equations [19], assuming fibre effective area from 66.5 to 86.6 μm^2 at 228.8 to 193.4 THz (1310 to 1550 nm). These results are shown as dashed lined Fig. 3(a) The modelling shows good agreement with the apparent fibre loss obtained experimentally, having an average difference of 0.18 dB.

IV. TRANSMISSION EXPERIMENT CHARACTERISATION

Fig. 5 shows the experimental system setup used for the transmission. This consisted of three test channels and amplified spontaneous emission (ASE) noise to fill 16.4 THz of bandwidth [20]. A total of 327×48 GBd wavelength division multiplexed (WDM) signals on a 50 GHz grid, starting at 220.83 THz (1357.57 nm) and ending at 237.13 THz (1264.25 nm) were emulated using spectrally shaped amplified spontaneous emission (SS-ASE) noise. The seed ASE noise source was an SLED which was amplified with a BDFA.
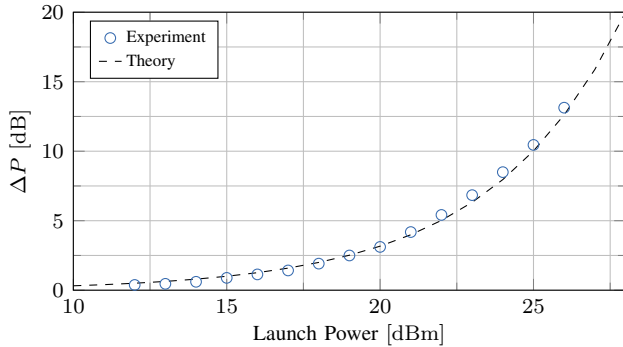
Fig. 4: Power transferred due to ISRS, measured as a function of the total input power for a fixed 16.4 THz bandwidth.

Each BDFA was a single-stage 250 metre bismuth-doped fibre (BDF), pumped by a 915 nm uncooled laser diode via 915 to 1150 nm Yb-fibre based wavelength converter, with a design similar to that described in [21]. All amplifiers except the receiver preamplifier were counter pumped and had a gain of >25.5 dB and a typical noise figure of 5.5 dB for 0 dBm input power. The pre-amplifier was co-pumped and had 22.5 dB gain and 4.8 dB noise figure for 0 dBm input power. Spectrum flattening was performed by a COHERENT WaveShaper® 4000B, which served as a WSS. This was used to control the input spectrum, add a notch for the test channels and combine with the channels under test.

The local oscillator (LO) and three carrier lasers had a linewidth of <500 kHz and the test channels were modulated with two 16QAM payloads based on random numbers generated by two different seeds, at a symbol rate of 48 GBd in an odd-even configuration. To aid in decoding, quadrature phase shift keyed (QPSK) pilot symbols were inserted at a rate of 1/32, and a header of 2^{10} symbols was used for synchronisation [22]. The entire frame was then root raised cosine (RRC) filtered with a roll-off of 0.01. Each IQ modulator was driven by an arbitrary waveform generator (AWG) at 128 GSa/s. Each set of test channels was then polarisation multiplexed using a 3 dB coupler, delay lines of 5 and 10 metres (for odd and even channels, respectively), both polarisation was recombined with a polarisation beam splitter and then odd and even channels combined with another 3 dB coupler. The central odd channel was used as the channel under test (CUT) for all the measurements. It is noted that the maximum variation of ZDF was around 1 THz but since this was in the last two reels of propagation, it is unlikely to contribute to much variation NLIN generation.

After transmission, the signals were amplified with a co-pumped BDFA and the CUT was selected using a band-pass filter with a 1.5nm bandwidth. After filtering, the signal was amplified again to maintain an optical power of 5 dBm at the coherent receiver. The electrical signals were digitised at 80 GSa/s and processed offline. First, frequency offset removal was performed on only the pilot symbols before downsampling the entire frame to 2 samples per symbol for RRC filtering. A 19-tap long filter was generated by the constant modulus algorithm, trained on the pilots before application to the

entire frame to recover the distorted signal. The frame was downsampled to 1 sample per symbol for the carrier recovery, phase was estimated from the pilots and the correction was applied to the entire frame. Finally, the payload signal was extracted and IQ orthogonalisation was performed before the bit error rate (BER), signal-to-noise ratio (SNR), generalised mutual information (GMI) and achievable information rate (AIR) were calculated. The AIR was calculated as the GMI of the payload minus the overhead from the inserted pilot symbols. No dedicated chromatic dispersion compensation step was performed and was entirely left to the equaliser to mitigate.

V. TRANSMISSION BANDWIDTH OPTIMISATION

To find the optimum launch power, both ISRS and NLIN near the ZDF must be taken into consideration. We used a fast ISRS integral GN model [16] considering the linear frequency dependence of the nonlinear coefficient γ from 1.8 to 2.2 /W/km at 220 to 238 THz. For SNR estimation, one preamplifer ASE noise contribution was considered as it is the dominant source of ASE in the system. From a launch power of 23 dBm, increasing the launch power by 1 dB results in more than 1 dB of additional power transfer, hence the mean apparent fibre loss across the transmission bandwidth would increase, leading to a lower overall system performance. During the optimisation process, the total launch power was fixed at 23 dBm and 20 attenuation points across the bandwidth were tuned for maximum capacity. The power for each channel was found by linearly interpolating from each of these attenuation points. This is shown in Fig. 7, which compares the ISRS mitigating, desired optimal and transmitted spectra. During the optimisation, it is assumed that the WSS can attenuate the BDFA output without the impact on BDFA gain. In addition, it is assumed that preamplifier gain will not be impacted. Experimentally, the optimised input power for each channel was obtained by using the WSS. The applied attenuation profile was only updated once and hence was unable to compensate for the nonlinear gain of the subsequent BDFA.

VI. RESULTS AND DISCUSSION

Back-to-back characterisation of the transceiver was performed by removing the fibre span and replacing it with a 20 dB optical attenuator. The SNR of the central channel was measured as the SS-ASE bandwidth load, as the three test channels and LO were swept from 220 to 238 THz. The results are shown in Fig. 8(a). The highest achieved back-to-back SNR from a WDM channel was 16.4 dB at 227.3 THz, showing the need for further optimisation of the entire transceiver chain compared with conventional C-band transceivers which can obtain SNRs >20 dB. The lowest SNR occurred at 221.04 THz. This frequency was where the gain of the BDFAs was not sufficient to overcome the loss, and the OSNR decreased. These channels are still viable for transmission over the fibre span, as the ISRS power transfer reduces the apparent fibre loss at these frequencies. Solid lines show the simulation results and markers, the experimental results for fixed 23 dBm launch power. The expected ASE
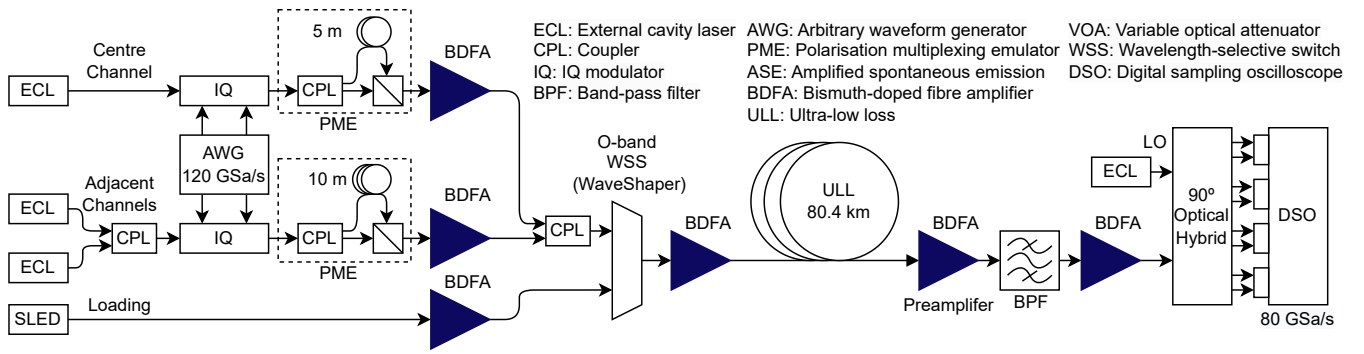
Fig. 5: Experimental setup for unrepeated transmission using WSS and BDFAs
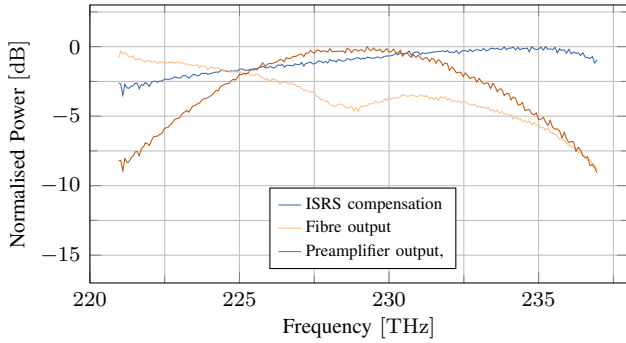

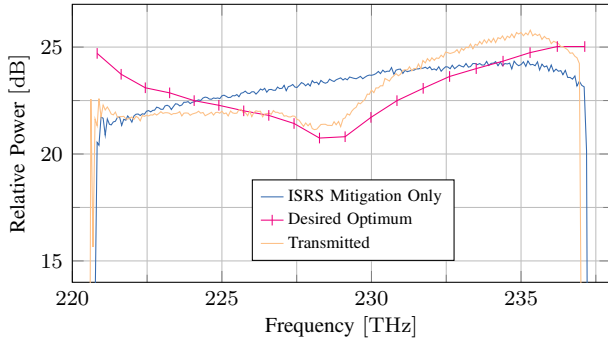Fig. 6: Optical spectra for flat input, post fibre transmission and after amplification.

Fig. 7: The launch spectra before and after optimisation, each having a total launch power of 23 dBm.

noise was calculated from the loss measured for 23 dBm launch power case shown in Fig. 2 where the gain of the BDFA was estimated from the powers before and after the preamplifier. The noise figure values were used from the profiles measured in Fig. 1. The NLIN was estimated using the model [16], where the evolution of the power along the fibre estimation shows good agreement with the measured results, as shown in Fig. 3(a). The SNR when considering only NLIN was also calculated and can be seen to cause a decrease in the SNR below that of the ASE around the ZDF. The total shows the expected SNR performance after combining the measured back-to-back, simulated ASE, and simulated NLIN. At the edges of the calculated transmission

spectrum, the model overestimates the SNR values, which is caused by missing contributions from other components in the transmission system.

The optimised launch power shown in Fig. 7 is highest at the higher frequencies, which helps with ISRS power transfer, and a reduced power in the middle of the spectrum, which improves NLIN. The transmission was performed with slightly different spectral power than the optimised one, as BDFA gain was not taken into account. This resulted in SNR gains mostly in channels at higher frequencies and a minimum gain at ZDF and lower frequencies, as can be observed from Fig. 8(b).

When the 80.4 km span was used for transmission, the input spectrum was set to ISRS mitigation only, and the total launch power values for the three channels were set to 21, 23 and 25 dBm (-3.1, -1.1 and 0.9 dBm/channel). The resultant SNR was measured as a function of frequency, and is shown in Fig. 8(b). The minimum SNR occurs at the highest frequency for both launch powers, where the combination of LO power, BDFA gain, fibre loss and ISRS power transfer are all in the worst condition. As the power increases, the impact of ISRS can be seen as the SNR increases for lower frequencies but decreases for higher frequencies.

In the centre of the transmission bandwidth, there is also a decrease in performance near the ZDF. This drop in performance is a function of launch power, and is measured compared to the channel at 224 THz to be 2.3, 2.5 and 3.9 dB for launch powers of 21, 23 and 25 dBm, respectively. The width of the drop is measured as the full width half maximum of the shape. The number of channels affected did not change monotonically with power, as the measured numbers of affected channels were 71, 76 and 75 channels, respectively.

The launch power per channel is then adjusted to mitigate the effects of FWM and ISRS as shown in Fig. 7 as transmitted and described by the optimisation procedure. The transmitted launch spectrum does not follow the desired optimum and so ideal performance increase was not observed. The loss in performance near the ZDF is also reduced to 2.0 dB, and the number of affected channels is reduced to 47 by the reduction in local launch power. The change in power around this channel improved the SNRs of the highest and lowest frequencies by 2 dB.

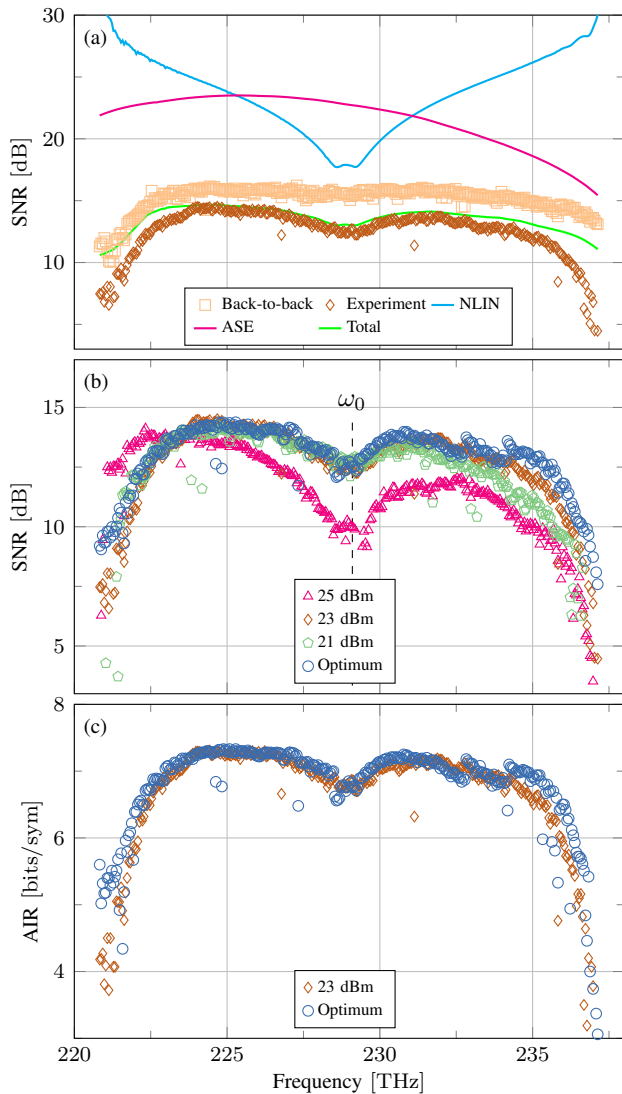The measured AIR as a function of frequency is shown

Fig. 8: (a) SNR from simulations and 23 dBm input (b) SNR from multiple input powers (c) achievable information rate measured for the channel under test as a function of frequency after transmission.

in Fig. 8(c). The total potential throughput is taken as the sum of every channel's GMI multiplied by the symbol rate, subtracting the rate of the pilot symbols. From these results, the maximum achievable throughput, assuming ideal FEC implementation, for the system with a simple ISRS compensating input spectrum, was calculated as 103.3 Tb/s and after optimisation, it improved to 106.0 Tb/s. This was an increase of 0.5 bits/sym for the channels at the edges of the spectrum.

VII. CONCLUSIONS

We have experimentally demonstrated ultrawideband DWDM coherent transmission over a single ultra-low loss span of 80.4 km, using only one type of doped fibre amplifier. We have experimentally corroborated the use of a model in O-band, which was used to optimise the launch power, in order to simultaneously overcome the inter-channel stimulated

Raman scattering and nonlinear interference noise near the zero dispersion frequency. This lead to a potential achievable throughput of 106 Tb/s without the use of any chromatic dispersion compensation. To the best of our knowledge, this work has achieved the highest single amplifier transmission bandwidth, 16.4 THz, for an unrepeated single-mode fibre link.

REFERENCES

[1] M. Filer, J. Gaudette, Y. Yin, D. Billor, Z. Bakhtiari, and J. L. Cox, "Low-margin optical networking at cloud scale," *Journal of optical communications and networking*, vol. 11, no. 10, pp. C94–C108, 2019.

[2] C. Xie and B. Zhang, "Scaling optical interconnects for hyperscale data center networks," *Proceedings of the IEEE*, vol. 110, no. 11, pp. 1699–1713, 2022.

[3] D. Tauber, B. Smith, D. Lewis, E. Muhigana, M. Nissov, D. Govan, J. Hu, Y. Zhou, J. Wang, W.-J. Jiang, R. Galeotti, F. Dell'Orto, and R. Siano, "Role of coherent systems in the next DCI generation," *J. Light. Technol*, vol. 41, no. 4, pp. 1139–1151, 2023. [Online]. Available: https://opg.optica.org/jlt/abstract.cfm?URI=jlt-41-4-1139

[4] T. Kato, H. Muranaka, S. Okada, Y. Tanaka, Y. Akiyama, T. Hoshida, Y. Wakayama, D. Soma, S. Beppu, D. J. Elson, N. Yoshikane, and T. Tsuritani, "Field-deployed fiber transmission of DWDM signal in S+ C+ L-band co-propagating with 400GBASE-LR8," *IEEE Photonics Technology Letters*, vol. 36, no. 1, pp. 16–19, 2023.

[5] D. Soma, T. Kato, S. Beppu, D. J. Elson, H. Muranaka, H. Irie, S. Okada, Y. Tanaka, Y. Wakayama, N. Yoshikane, T. Hoshida, and T. Tsuritani, "25-THz O+ S+ C+ L+ U-band digital coherent DWDM transmission using a deployed fibre-optic cable," in *49th European Conference on Optical Communications (ECOC 2023)*, vol. 2023. IET, 2023, pp. 1658–1661.

[6] B. J. Puttnam, R. S. Luís, Y. Huang, I. Phillips, D. Chung, N. K. Fontaine, B. Boriboon, G. Rademacher, M. Mazur, L. Dallachiesa *et al.*, "321 Tb/s E/S/C/L-band transmission with E-band bismuth-doped fiber amplifier and optical processor," *Journal of Lightwave Technology*, 2024.

[7] B. J. Puttnam, R. S. Luís, I. Phillips, M. Tan, A. Donodin, D. Pratiwi, L. Dallachiesa, Y. Huang, M. Mazur, N. Fontaine, H. Chen, D. Chung, V. Ho, D. Orsuti, B. Boriboon, G. Rademacher, L. Palmieri, R. Man, R. Ryf, D. T. Neilson, W. Forysiak, and H. Furukawa, "402 Tb/s GMI data-rate OESCLU-band transmission," in *Optical Fiber Communication Conference*. Optica Publishing Group, 2024, pp. Th4A–3.

[8] B. P. 1, R. S. Luís, I. Phillips, M. Tan, A. Donodin, D. Pratiwi, L. Dallachiesa, Y. Huang, M. Mazur, N. Fontaine, H. Chen, D. Chung, V. Ho, D. Orsuti, D. A. Shaji, B. Boriboon, G. Rademacher, L. Pallmieri, R. Man, R. Ryf, D. Neilson, W. Forysiak, H. Furukawa, and C. Antonelli, "339.1 tb/s oesclu-band transmission over 100 km smf," in *Optical Fiber Communication Conference*. IEEE, 2024, p. M2B.2.

[9] J. Renaudier, A. C. Meseguer, A. Ghazisaeidi, P. Tran, R. R. Muller, R. Brenot, A. Verdier, F. Blache, K. Mekhazni, B. Duval *et al.*, "First 100-nm continuous-band WDM transmission system with 115Tb/s transport over 100km using novel ultra-wideband semiconductor optical amplifiers," in *2017 European Conference on Optical Communication (ECOC)*. IEEE, 2017, pp. 1–3.

[10] A. Khegai, Y. Ososkov, S. Firstov, K. Riumkin, S. Alyshev, A. Kharakhordin, A. Lobanov, A. Guryanov, and M. Melkumov, "O+ E band BDFA with flattop 116 nm gain bandwidth pumped with 250 mW at 1256 nm," in *Optical Fiber Communication Conference*. Optica Publishing Group, 2021, pp. Tu1E–4.

[11] Y. Wakayama, D. J. Elson, V. Mikhailov, R. Maneekut, J. Luo, N. Yoshikane, D. Inniss, and T. Tsuritani, "400GBASE-LR4 and 400GBASE-LR8 transmission reach maximization using bismuth-doped fiber amplifiers," *Journal of Lightwave Technology*, vol. 41, no. 12, pp. 3908–3915, Jun. 2023. [Online]. Available: https://doi.org/10.1109/jlt.2023.3269536

[12] A. Ferrari *et al.*, "Assessment on the achievable throughput of multi-band ITU-T G.652.D fiber transmission systems," *J. Light. Technol*, vol. 38, no. 16, pp. 4279–4291, 2020. [Online]. Available: https://doi.org/10.1109/jlt.2020.2989620

[13] P. Poggiolini *et al.*, "Closed form expressions of the nonlinear interference for UWB systems," in *ECOC 2022*, 2022, tu1D.1. [Online]. Available: https://opg.optica.org/abstract.cfm?URI=ECEOC-2022-Tu1D.1

[14] D. J. Elson, Y. Wakayama, V. Mikhailov, J. Luo, N. Yoshikane, D. Inniss, and T. Tsuritani, "9.6-THz single fibre amplifier O-band coherent DWDM transmission," in *Optical Fiber Communication*

Conference (OFC) 2023. Optica Publishing Group, 2023, p. Th4B.4. [Online]. Available: https://doi.org/10.1364/ofc.2023.th4b.4

[15] D. J. Elson, V. Mikhailov, J. Luo, S. Beppu, G. Baxter, R. Stolte, L. Stewart, S. Takasaka, M. Jarmolovičius, E. Sillekens, R. I. Killey, P. Bayvel, N. Yoshikane, T. Tsuritani, , and Y. Wakayama, "Continuous 16.4-THz bandwidth coherent DWDM transmission in O-band using a single fibre amplifier system," in *Th4A.2, OFC*, 2024.

[16] M. Jarmolovičius, D. Semrau, H. Buglia, M. Shevchenko, F. M. Ferreira, E. Sillekens, P. Bayvel, and R. I. Killey, "Optimising O-to-U Band Transmission Using Fast ISRS Gaussian Noise Numerical Integral Model," *Journal of Lightwave Technology*, pp. 1–8, 2024.

[17] G. Saavedra, M. Tan, D. J. Elson, L. Galdino, D. Semrau, M. A. Iqbal, I. D. Phillips, P. Harper, A. Ellis, B. C. Thomsen *et al.*, "Experimental analysis of nonlinear impairments in fibre optic transmission systems up to 7.3 thz," *Journal of Lightwave Technology*, vol. 35, no. 21, pp. 4809–4816, 2017.

[18] D. Semrau, R. I. Killey, and P. Bayvel, "The gaussian noise model in the presence of inter-channel stimulated Raman scattering," *Journal of Lightwave Technology*, vol. 36, no. 14, pp. 3046–3055, 2018.

[19] M. Jarmolovičius, H. Buglia, E. Sillekens, P. Bayvel, and R. Killey, "Ultrawideband optical fibre throughput in the presence of total optical power constraints from C to OESCLU spectral bands," in *2024 European Conference on Optical Communication (ECOC)*. IEEE, 2024, p. M3B.2.

[20] D. J. Elson, G. Saavedra, K. Shi, D. Semrau, L. Galdino, R. Killey, B. C. Thomsen, , and P. Bayvel, "Investigation of bandwidth loading in optical fibre transmission using amplified spontaneous emission noise," *Opt. Express*, vol. 25, no. 16, pp. 19 529–19 537, Aug 2017. [Online]. Available: https://opg.optica.org/oe/abstract.cfm?URI=oe-25-16-19529

[21] V. Mikhailov, Y. Sun, J. Luo, F. Khan, D. Inniss, Y. Dulashko, M. Lee, J. Mann, R. S. Windeler, P. S. Westbrook *et al.*, "1255-1355 nm (17.6 THz) bandwidth O-band BDFA pumped using uncooled multimode 915 nm laser diode via YDF conversion stage." *Journal of Lightwave Technology*, 2023.

[22] Y. Wakayama, T. Gerard, E. Sillekens, L. Galdino, D. Lavery, R. I. Killey, and P. Bayvel, "2048-QAM transmission at 15 GBd over 100 km using geometric constellation shaping," *Optics Express*, vol. 29, no. 12, pp. 18 743–18 759, 2021.